Regularized Plane-wave Least-squares Kirchhoff Migration

Xin Wang[1 2], *Wei Dai*[1 2] *and Gerard T. Schuster*[1]
[1]*King Abdullah University of Science and Technology*
[2]*University of Utah*

SUMMARY

A Kirchhoff least-squares migration (LSM) is developed in the prestack plane-wave domain to increase the quality of migration images. A regularization term is included that accounts for mispositioning of reflectors due to errors in the velocity model. Both synthetic and field results show that: 1) LSM with a reflectivity model common for all the plane-wave gathers provides the best image when the migration velocity model is accurate, but it is more sensitive to the velocity errors, 2) the regularized plane-wave LSM is more robust in the presence of velocity errors, and 3) LSM achieves both computational and IO saving by plane-wave encoding compared to shot-domain LSM for the models tested.

INTRODUCTION

It has been shown that least-squares migration (Nemeth et al., 1999; Duquet et al., 2000) can provide better quality images than Kirchhoff Migration (KM) if an accurate migration velocity is used. However, one of the drawbacks of LSM is its high computational cost. Romero et al. (2000) proposed a blended source method for contentional migration by encoding and stacking different shot gathers into a supergather This algorithm can be applied to LSM with Kirchhoff migration (Dai et al., 2011; Wang and Schuster, 2012), wave-equation migration (Huang and Schuster, 2012) and reverse time migration (Dai et al., 2010). Wave-equation LSM can achieve high computational efficiency (Dai et al., 2011; Huang and Schuster, 2012) by modeling and migrating the supergather with one finite-difference solution to the wave equation for a large distribution o encoded point sources. For Kirchhoff LSM, however, the computational cost is determined by the total number of traces, which cannot be decreased by the blended encoding of shot gathers. As a less expensive alternative, a linear time-shift phase encoding which is identical to the tau-p transform, can transfer the shot-domain data to the plane-wave domain. By replacing the large number of shots with a smaller number of ray parameters, a significant computational saving is achieved for Kirchhoff LSM. Our empirical tests show that plane-wave KLSM is about 3 times more expensive than KM, and 7 times less expensave than standard KLSM for the models tested.

Due to velocity model errors, reflectors from different plane-wave gathers can be positioned differently, so stacking the prestack migration images will blur the image of the interfaces. To overcome this problem, individual migration images are computed for different plane-wave gathers. Since the images from two plane-wave gathers with slightly different incidence angles are similar, a regularization term is applied to encourage their similarities. In addition, the prestack images provide enhanced opportunities for velocity analysis.

This paper is organized into the following three sections. The first part presents the theory of regularized plane-wave least-squares migration (RPLSM). The next section presents synthetic and field data results that demonstrate the efficiency and effectiveness of RPLSM. Finally, a summary is provided.

THEORY

The first step in RPLSM is to apply a linear time shift to the shot gathers and sum them up to form the response to an incident plane wave with a specified p value. Assuming a 2D survey geometry, the encoding process is expressed as:

$$d(x_g,t;p) = \sum_{x_s} d(x_g,t;x_s) * \delta(t - p \cdot x_s), \tag{1}$$

where the shot-domain data $d(x_g,t;x_s)$ are encoded with a time-shift function $\delta(t-p\cdot x_s)$ and stacked together. The time shift $p \cdot x_s$ is a linear function of source position x_s, and p is the ray parameter defined as $p = \frac{sin\theta}{v}$, where θ is the surface shooting angle and v is the velocity at the surface.

Assuming the reflectivity model $\mathbf{m}$ is independent of the ray parameter, for a dataset with N_p plane-waves the modeling operation can be expressed as

$$\begin{bmatrix} \mathbf{d}_1 \\ \mathbf{d}_2 \\ \cdot \\ \mathbf{d}_{N_p} \end{bmatrix} = \begin{bmatrix} \mathbf{L}_1 \\ \mathbf{L}_2 \\ \cdot \\ \mathbf{L}_{N_p} \end{bmatrix} [\mathbf{m}], \tag{2}$$

and the migration operation can be expressed as

$$\mathbf{m}_{mig} = \left[\mathbf{L}_1^T \ \mathbf{L}_2^T \ \cdot \ \mathbf{L}_{N_p}^T\right] \begin{bmatrix} \mathbf{d}_1 \\ \mathbf{d}_2 \\ \cdot \\ \mathbf{d}_{N_p} \end{bmatrix} = \sum_{i=1}^{N_p} \mathbf{L}_i^T \mathbf{d}_i, \tag{3}$$

where the final image is the stack of migration images from all of the individual plane-waves gathers. Here $\mathbf{d_i}$ ($\mathbf{L_i}$) represents the response of the system to (modeling operator for) the plane-wave source with the ith ray parameter. PLSM is formulated to find the $\mathbf{m}$ that minimizes the misfit functional

$$f(\mathbf{m}) = \frac{1}{2}\sum_{i=1}^{N_p} ||\mathbf{L}_i\mathbf{m} - \mathbf{d}_i||^2 + \mathbf{R}, \tag{4}$$

where $\mathbf{R}$ is the regularization term, and $\mathbf{m}$ is defined as the stacked migration image. If the migration velocity is not accurate, the prestack images from different plane-wave gathers are dissimilar and simple stacking will blur the image and slow the convergence.

In order to improve the robustness of plane-wave LSM in the presence of migration velocity errors, we assume each plane-wave gather $\mathbf{d_i}$ is associated with its own reflectivity model $\mathbf{m_i}$,

DOI http://dx.doi.org/10.1190/segam2013-0278.1

so an ensemble of prestack images $\widehat{\mathbf{m}}$ can be defined as

$$\widehat{\mathbf{m}} = \begin{bmatrix} \mathbf{m}_1 \\ \mathbf{m}_2 \\ \cdot \\ \mathbf{m}_{N_p} \end{bmatrix}, \tag{5}$$

so the modeling and migration equations can be expressed as

$$\begin{bmatrix} \mathbf{d}_1 \\ \mathbf{d}_2 \\ \cdot \\ \mathbf{d}_{N_p} \end{bmatrix} = \begin{bmatrix} \mathbf{L}_1 & & & \\ & \mathbf{L}_2 & & \\ & & \cdot & \\ & & & \mathbf{L}_{N_p} \end{bmatrix} \begin{bmatrix} \mathbf{m}_1 \\ \mathbf{m}_2 \\ \cdot \\ \mathbf{m}_{N_p} \end{bmatrix}, \tag{6}$$

and

$$\begin{bmatrix} \mathbf{m}_{mig,1} \\ \mathbf{m}_{mig,2} \\ \cdot \\ \mathbf{m}_{mig,N_p} \end{bmatrix} = \begin{bmatrix} \mathbf{L}_1^T & & & \\ & \mathbf{L}_2^T & & \\ & & \cdot & \\ & & & \mathbf{L}_{N_p}^T \end{bmatrix} \begin{bmatrix} \mathbf{d}_1 \\ \mathbf{d}_2 \\ \cdot \\ \mathbf{d}_{N_p} \end{bmatrix}. \tag{7}$$

For simplicity, we define $\widehat{\mathbf{L}}$ as the forward modeling operator for all the plane-wave gathers

$$\widehat{\mathbf{L}} = \begin{bmatrix} \mathbf{L}_1 & & & \\ & \mathbf{L}_2 & & \\ & & \cdot & \\ & & & \mathbf{L}_{N_s} \end{bmatrix}, \tag{8}$$

so that equations 6 and 7 can be rewritten in compact form

$$\mathbf{d} = \widehat{\mathbf{L}}\widehat{\mathbf{m}}, \tag{9}$$

$$\widehat{\mathbf{m}}_{\mathbf{mig}} = \widehat{\mathbf{L}}^{\mathbf{T}}\mathbf{d}. \tag{10}$$

Therefore, the misfit functional with the ensemble of prestack images is defined as

$$\begin{aligned} f(\widehat{\mathbf{m}}) &= \frac{1}{2}\sum_{i=1}^{N_p} ||\mathbf{L}_i\mathbf{m}_i - \mathbf{d}_i||^2 + \mathbf{R}, \\ &= \frac{1}{2}||\widehat{\mathbf{L}}\widehat{\mathbf{m}} - \mathbf{d}||^2 + \mathbf{R}. \end{aligned} \tag{11}$$

The regularization term $\mathbf{R}$ is defined as a function to penalize the difference between migration images computed with slightly different incidence angles, and it is defined as

$$\mathbf{R} = \frac{1}{2}\gamma \sum_{i=1}^{N_p-1} ||\frac{\mathbf{m}_{i+1}}{\lambda_{i+1}} - \frac{\mathbf{m}_i}{\lambda_i}||^2, \tag{12}$$

where λ_i is the normalization parameter to make the amplitudes of $\mathbf{m_i}$ and $\mathbf{m_{i+1}}$ relatively equal, and γ is the damping coefficient that is chosen by trial-and-error testing. We denote this regularized plane-wave LSM as regularized plane-wave least-squares migration (RPLSM).

NUMERICAL RESULTS

Synthetic Data Test

Synthetic data are generated for the 2D Marmousi2 model. The model size is 1501 $\times$ 501, and the grid interval is 5 m, with 301 shot gathers and a shot interval of 25 m, and each shot gather is recorded with 750 receivers with the interval 10 m. Forty-five plane-wave gathers are generated by the $\tau - p$ transform, with a range of ray parameters between -0.47 ms/m and 0.47 ms/m. To test the robusness of this algorithm, an erroneous velocity model with a maximum of 5% error is used for the migration velocity. The velocity error will shift reflector positions by 2 and 2.5 wavelengths at the respective depths of 1.5 and 2 km.

Figures 1a and 1b show the 45 plane-wave gather and 301 common shot gather (CSG) KM images. The PKM image is almost identical to that of the CSG-domain KM, which means the 45 plane-waves are sufficient for imaging the subsurface structure accurately. By replacing 301 CSGs with 45 plane-wave gathers, a computational speed up of $\frac{301}{45} = 6.69$ is achieved, and this efficiency can be further improved by decreasing the number of plane-waves. However, the image quality can be damaged by an insufficient number of plane-wave angles. Stork and Kapoor (2004), Etgen (2005) and Zhang et al. (2005) provided an estimate of how many angles are needed as a function of recording aperture, velocity model, and the estimated dip-angle of the reflectors.

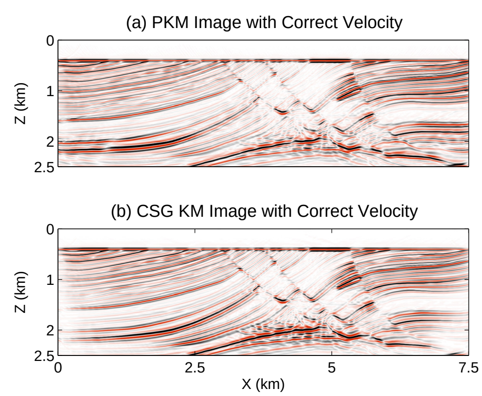

Figure 1: Kirchhoff migration images with the accurate velocity model of: (a) 31 plane-wave gathers and (b) 45 CSGs (shot positions are evenly distributed.

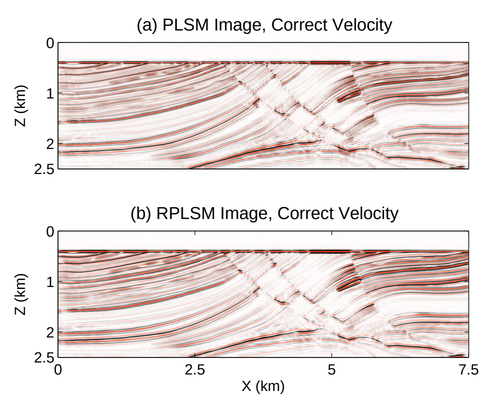

Figure 2: LSM images with accurate velocity model after 10 iterations: (a) PLSM and (b) RPLSM.

DOI http://dx.doi.org/10.1190/segam2013-0278.1

Figures 2a and 2b show the PLSM and the RPLSM images after 10 iterations. Both of them are of better quality than the PKM (Figure 1a). It is also noticed that when the migration velocity is accurate, PLSM provides a high resolution image and has a better convergence (Figure 5) than RPLSM because the prestack images are consistent. Hence, stacking PKM images together can suppress the migration artifacts.

The sensitivity of the migration images with respect to errors in the velocity model is now tested. Figure 3a-3c show the PKM, PLSM and RPLSM images with the erroneous migration velocity. The PLSM image has the highest resolution at the shallow depth because there is no velocity error here, but for the deep part (circled) RPLSM provides the best image.

Common image gathers (CIG) from PKM and RPLSM are compared in Figure 4. Several areas marked with the green gashed lines are selected to show the advantages of RPLSM.

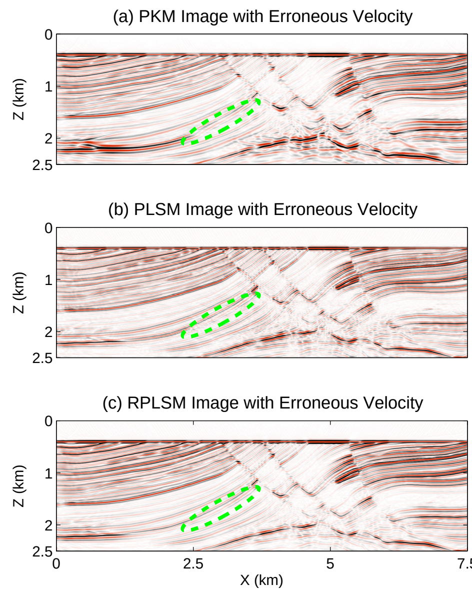

Figure 3: Migration images with erroneous velocity model of: (a) PKM, (b) PLSM and (c) RPLSM after 10 iterations.

Figure 5 shows the misfit vs iteration plots of PLSM and RPLSM with both the true and erroneous migration velocity. When the velocity is accurate, PLSM has a better convergence rate. If the velocity is not accurate, RPLSM converges faster than PLSM.

Marine Data Test

The proposed methods are tested on 2D marine data. There are 515 shots with a shot interval of 37.5 m, and each shot is recorded by a 6 km long cable with 480 receivers and a 12.5 m hydrophone interval. The nearest receiver offset from the source is 198 m. The CSGs are first transformed into common midpoint profiles (CMPs), then a normal moveout time shift is applied followed by a 2D interpolation. The interpolated data are then transformed into common receiver gathers (CRG) with a split-spread acquisition geometry using reciprocity. A tau-p transform is applied to each CRG to generate 31 plane-wave gathers with ray parameters (p) ranging

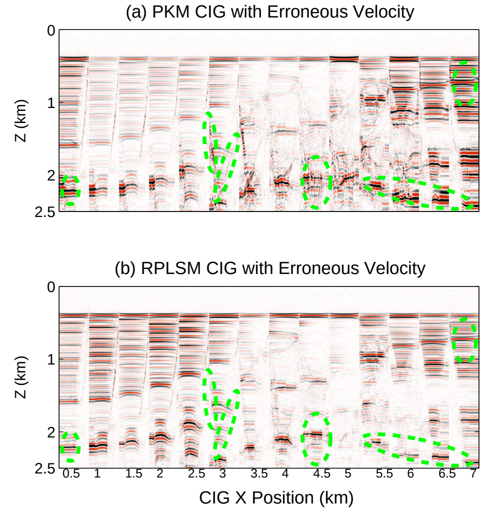

Figure 4: CIGs with erroneous velocity for: (a) PKM and (b) RPLSM after 10 iterations.

from -0.333 ms/m to 0.333 ms/m with an even sampling in p, and each plane-wave gather has 1260 receivers. The source wavelet is estimated by stacking traces with a strong water bottom reflection. Waveform inversion (Altheyab, 2012) is used to get the migration velocity model and the model size is 2519 $\times$ 581 with a gridpoint interval of 6.25 m.

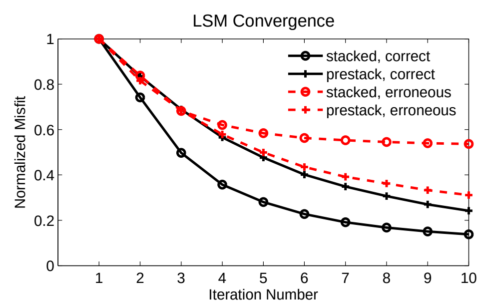

Figure 5: Data misfit function vs iteration number plots for PLSM and RPLSM for the true and erroneous migration velocities. Black lines are for the accurate migration velocity model and red lines are the for the erroneous velocity model.

Figures 6(a)-6(d) shows, respectively, the CSG KM, PKM, PLSM and RPLSM images. The image quality of CSGKM and PKM are comparable, and the shallow reflectors are highly resolved with PKM, while the deep part contains more artifacts. Figure 7 shows the two zoom views of PKM, PLSM and RPLSM images which are marked as boxes in Figure 6. Similar to the synthetic results, Figure 7a-7c show that at the shallow parts both the PLSM and RPLSM images are of better quality than the KM image, but the PLSM image has slightly higher quality than the RPLSM image which indicates the velocity at shallow depth is accurate. However, for the deep part (as shown in Figure 7d-7f), the PLSM image shows a much higher level of noise, and the RPLSM provides a better quality image with fewer artifacts and shows more continuous re-

DOI http://dx.doi.org/10.1190/segam2013-0278.1

flectors but with lower resolution. For comparison, the image quality of PKM is the best among the three.

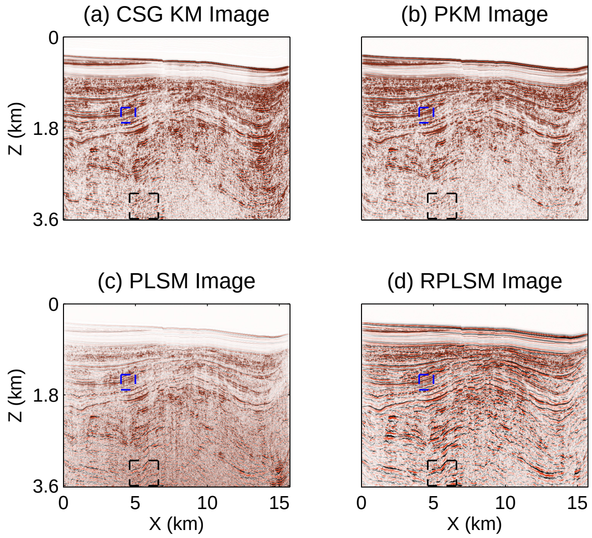

Figure 6: Migration images of: (a) CSG domain KM, (b) PKM, (c) PLSM and (d) RPLSM.

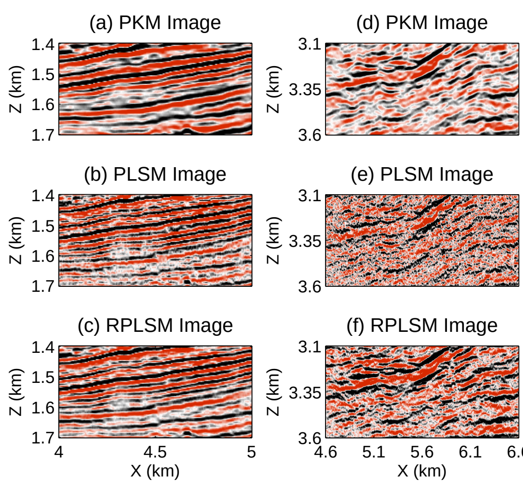

Figure 7: Zoom views of PKM, PLSM and RPLSM images. (a)-(c) are the zoom views of the blue box and (d)-(f) show the zoom views of the black box.

By analyzing the CIGs of PKM and RPLSM (Figure 8a and 8b), it is found that RPLSM increases the prestack image resolution more than KM; but after stacking the final image is blurred which is a symptom of an inaccurate velocity model. A trim statics technique may be needed to provide a better stacked image. In addition, the high-resolution prestack images can be used to correct the velocity model by migration velocity analysis.

Figure 9 shows the plots of residual vs iteration number for these two LSM methods. PLSM provides a reflectivity model to reduce the RMS misfit value to 55%, compared to 30% for RPLSM. The computational and IO cost of RPLSM and PLSM are about $\frac{31\times1260}{515\times480} = 0.158$ of that for shot domain LSM.

DISCUSSION AND CONCLUSION

A plane-wave least-squares migration algorithm is proposed to efficiently produce high quality images. By transforming CSG data into the plane-wave domain data, the computation and IO costs are significantly decreased. Synthetic and field results show that PLSM can provide high quality images when the migration velocity is accurate. The success of PLSM vanishes when the migration velocity model contains significant errors. To improve the robustness of this algorithm, a regularized plane-wave least-squares migration method is proposed and shown to give the most focused images in the presence of migration velocity errors. In addition, the prestack CIGs provides enhanced opportunities for velocity analysis.

ACKNOWLEDGMENTS

We thank the CSIM members for supporting this research, and we also thank the High Performance Computational Center and IT support at KAUST.

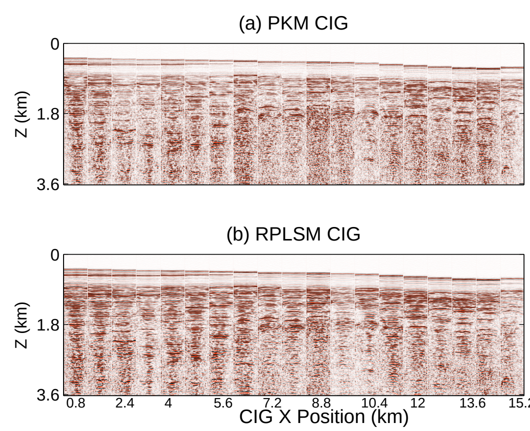

Figure 8: CIGs of (a) PKM and (b) RPLSM after 10 iterations.

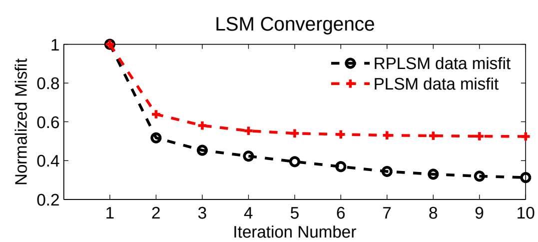

Figure 9: Convergence of PLSM and RPLSM for the marine data test.

DOI http://dx.doi.org/10.1190/segam2013-0278.1

http://dx.doi.org/10.1190/segam2013-0278.1

EDITED REFERENCES

Note: This reference list is a copy-edited version of the reference list submitted by the author. Reference lists for the 2013 SEG Technical Program Expanded Abstracts have been copy edited so that references provided with the online metadata for each paper will achieve a high degree of linking to cited sources that appear on the Web.

REFERENCES

Altheyab, A., 2012, Hybrid linear and nonlinear waveform inversion of marine data: CSIM Annual Report, 1–5.

Dai, W., C. Boonyasiriwat, and G. T. Schuster, 2010, Three-dimensional multisource least-squares reverse time migration: 80th Annual International Meeting, SEG, Expanded Abstracts, **29**, 3120–3124.

Dai, W., X. Wang, and G. T. Schuster, 2011, Least-squares migration of multisource data with a deblurring filter: Geophysics, **76**, no. 5, R135–R146, http://dx.doi.org/10.1190/geo2010-0159.1.

Duquet, B., K. J. Marfurt, and J. A. Dellinger, 2000, Kirchhoff modeling, inversion for reflectivity, and subsurface illumination: Geophysics, **65**, 1195–1209, http://dx.doi.org/10.1190/1.1444812.

Etgen, J. T., 2005, How many angles do we really need for delayed-shot migration?: 75th Annual International Meeting, SEG, Expanded Abstracts, **24**, 1985–1988.

Huang, Y., and G. T. Schuster, 2012, Multisource least-squares migration of marine streamer and land data with frequency- division encoding: Geophysical Prospecting, **60**, no. 4, 663–680, http://dx.doi.org/10.1111/j.1365-2478.2012.01086.x.

Nemeth, T., C. Wu, and G. T. Schuster, 1999, Least-squares migration of incomplete reflection data: Geophysics, **64**, 208–221, http://dx.doi.org/10.1190/1.1444517.

Romero, L. A., D. C. Ghiglia, C. C. Ober, and S. A. Morton, 2000, Phase encoding of shot records in prestack migration: Geophysics, **65**, 426–436, http://dx.doi.org/10.1190/1.1444737.

Stork, C., and J. Kapoor, 2004, How many p-values do you want to migrate for delayed shot wave equation migration?: 74th Annual International Meeting, SEG, Expanded Abstracts, 1041–1044.

Wang, X., and G. T. Schuster, 2012, Multisource least-squares migration of marine data: 82nd Annual International Meeting, SEG, Expanded Abstracts, **31**, 1–5.

Zhang, Y., J. Sun, C. Notfors, S. H. Gray, L. Chernis, and J. Young, 2005, Delayed-shot 3D depth migration: Geophysics, **70**, no. 5, E21–E28. http://dx.doi.org/10.1190/1.2146078.